Characterization of the Benefit of APS Flash Coatings in Improving TBC Lifetime

Bruce A. Pint[1], Michael J. Lance[1], Ercan Cakmak[1], Kenneth A. Kane[1], J. Allen Haynes[1], Edward J. Gildersleeve[2], Sanjay Sampath[2]

(1) Materials Science & Technology Division, Oak Ridge National Laboratory, Oak Ridge, TN
pintba@ornl.gov (corresponding), lancem@ornl.gov, cakmake@ornl.gov, kaneka@ornl.gov, haynesa@ornl.gov
(2) Center for Thermal Spray Research, Stony Brook University, Stony Brook, NY
edward.gildersleeve@stonybrook.edu, sanjay.sampath@stonybrook.edu

Abstract

The addition of an air plasma sprayed (APS) "flash" layer on top of a high velocity oxygen fuel (HVOF) bond coating has been shown to extend the lifetime of thermal barrier coatings. A series of furnace cycle tests (FCTs) has been conducted at 1100 °C in air + 10 % H_2O to study the benefit of flash coatings on rod and disk alloy 247 specimens and provide a better mechanistic understanding of their benefit. Flash coatings of NiCoCrAlY and NiCoCrAlYHfSi both improved the FCT lifetime of rod specimens tested in 100-hr cycles and disk specimens tested in 1-hr cycles. In 1-hr cycles, the NiCoCrAlY flash coating significantly outperformed an HVOF-only NiCoCrAlYHfSi bond coating and a NiCoCrAlYHfSi flash coating. Both flash coatings increased the bond coating roughness compared to HVOF. During exposure, the flash layer formed an intermixed alumina-metal layer that appeared to inhibit crack formation. Using a time series of observations, the lower Y+Hf content in the Y-only flash coating appeared to reduce Al consumption. The HVOF layer acted as a source of Al for the adjacent mixed zone. A second series of specimens included a fully APS bond coating where oxide had penetrated through the entire coating to the substrate after only 100, 1-hr cycles and lifetime was similar to an HVOF-only bond coating. The inner HVOF layer with the outer APS flash coating prevented this complete penetration from occurring.

Keywords

Thermal barrier coatings, APS flash coating, furnace cycle testing

Introduction

Natural gas-fired simple and combined cycle power generation will continue to be the largest source of electricity in the US for the foreseeable future [1]. The traditional goal is increasing turbine efficiency to lower both emissions and the cost of electricity. Higher turbine inlet temperatures are often the clearest path to increasing efficiency of the Brayton cycle. However, higher temperatures accelerate degradation thereby impacting durability and reliability, which are paramount for utilities and consumers. One concern about today's industrial gas turbines (IGTs) is that they could be a stranded asset in a low-carbon future where fossil fuel combustion is minimized. A potential alternative is that IGTs will be used to burn "green" hydrogen generated using renewables [2,3]. The challenges with this idea include the storage, handling and combustion of H_2. For high temperature materials, there will be new challenges associated with the lower energy density and 5-10 % higher flame temperature of H_2 combustion [2]. To maintain the turbine output compared to natural gas combustion, the temperature will increase, which again will be a challenge for maintaining durability.

For the turbine hot section, a key materials technology for durability and higher temperature superalloy performance is thermal barrier coatings (TBCs) [4-6]. With the deployment of TBCs in IGTs over the past several decades there has been considerable development and optimization of TBCs for this particular application where the components are considerably larger than aero-engines [7-10]. Focusing on sprayed coatings for IGT applications, there has been limited progress in the past decade in terms of new bond coatings. One strategy that has emerged in the literature and in production is the use of a metallic "flash" air plasma sprayed (APS) NiCoCrAlY layer on top of a high velocity oxygen fuel (HVOF) bond coating [11-15]. In furnace cycle testing (FCT), flash coatings have been shown to extend the lifetime of ceramic APS Y_2O_3-stabilized ZrO_2 (YSZ) top coatings particularly for rod specimens. This paper reviews a number of the flash coating FCT results that have been generated at Oak Ridge National Laboratory (ORNL) on flash coatings over the past 4 years and some work that is currently in progress. The results focus on lower cost, polycrystalline superalloy 247 (trade name Mar-M247) substrates and FCT testing in air with 10 % H_2O. The presence of water vapor and its detrimental effect on high temperature oxidation [1,16-24] will be particularly important for H_2 combustion.

The current results question the conclusion that flash coatings are effective because of their higher roughness compared to bond coatings without a flash coating and indicates that NiCoCrAlYHfSi powder compositions that are effective for HVOF-only bond coatings are not the best choice for the APS flash layer.

Experimental Procedure

Rod (12.5 mm diameter, ~30 mm length) and disk (2 mm thick, ~16 mm diameter with chamfered edges) specimens machined from superalloy 247 (composition in Table 1) were grit blasted with alumina prior to coating using standard, air-plasma spray (APS) and high velocity oxygen fuel (HVOF) processes [15]. The two powder compositions also are shown in Table 1 and both APS and HVOF used a 16-88 µm powder size. After the bond coating was deposited, the substrates were annealed in a vacuum of 10^{-4} Pa (10^{-6} Torr) for 4 hr at 1080 °C. After annealing, the disks were coated with ~200 µm of "standard" APS YSZ with a porosity of 17.1±0.5 % and the rods were coated with ~300 µm of higher porosity (20.4±1.4%) APS YSZ [25,26]. Roughness measurements were previously reported.

Groups of 3-5 similarly-coated specimens were exposed to determine average FCT lifetimes of rod or disk specimens at each condition. Coating failure occurred when the entire YSZ spalled from the disks or the coating on the rods cracked along the length. All of the FCT experiments were conducted at 1100 °C in air with 10±1 vol. % H_2O. Injected water was atomized into dry, filtered air flowing at 500 ml/min. For 1-hr cycles, the specimens were hung from alumina rods and attached with Pt-Rh wire in an automated cyclic rig. Specimens were cooled in laboratory air for 10 min to <30 °C between cycles and were weighed and inspected every 20 cycles (once per day). For 100-hr cycles, the specimens were held in an alumina boat and heated slowly to temperature (~4 hr) in a tube furnace with an alumina reaction tube. The specimens were heated and cooled in flowing argon. Specimens were cooled to room temperature for inspection and weighed using a Mettler-Toledo model XP205 balance, however, only time to failure is reported here.

Residual stress in the alumina scale [27] was measured using a Dilor XY800 Raman microprobe (Horiba Scientific, Edison, NJ) with an Innova 308c Ar+ laser (Coherent, Inc., Santa

Clara, CA) operating at 5145 Å with a power of 10 mW at the YSZ surface and a laser spot size of 10µm. Photo-stimulated luminescence piezospectroscopy (PLPS) stress maps were collected on the flat specimens and a line profile was collected along the length of rod specimens. The acquisition time for one spectrum was 0.1-0.5 s and 3,468 and 2001 spectra were collected from the disk and rod specimens, respectively. A time series of measurements was conducted at the same location using an established procedure for collection and data analysis [23]. Only a single stress was fitted to each spectrum due to the large number collected.

Representative specimens were mounted in epoxy and polished for examination by light microscopy and scanning electron microscopy (SEM) equipped with an energy dispersive X-ray spectrometer (EDS). Time series of disk specimens were created by cutting off portions of the disk after 0, 100, 300 and 500 cycles. Micro X-ray computed tomography (µXCT) was performed using a Zeiss Xradia Versa 520 XCT system operated at 160 kV and 62.7 µA (10W). This particular unit uses both geometric and optical magnification (using scintillator objectives in front of a CCD camera) to obtain the desired resolution. The scans were performed in a 2-step fashion. First, a large area was scanned using the 4x objective and then a zoomed-in scan was performed with the 20x objective to focus on an area of interest. The pixel sizes were 1.19 µm and 0.503 µm using a 1x1 and 2x2 binning on the camera for the 4x and 20x scans, respectively. For image processing, segmentation and quantification, the ORS Dragonfly PRO v.3.5 software was used. A non-local means smoothing filter was used to reduce the noise in the data while preserving the shape and size of the defects [28]. The segmentation process involved selection of a region of X-ray absorption intensities to define an area of interest (e.g., metal vs. air). Any pixel within the selected intensity range is then marked (and colored) to belong to a region of interest (ROI). Within a ROI, one can then perform a connectivity analysis where neighboring voxels (volumetric pixel) are marked to belong to a single element (i.e. phase). In other words, if there is no connection between two voxels of the ROI, they belong to two separate elements. These elements can then be classified according to their volumes (number of voxels an element occupies x volume of a voxel). For this particular study, the connectivity analysis was used to determine if there were any disconnected (i.e., floating) metal particles within the oxide layer.

Table 1. Alloy chemical composition (mass %, balance Ni) determined by plasma and combustion analyses.

Alloy	Cr	Al	Co	Ti	Hf	Y	S*	Other
247	8.5	5.7	9.8	1.0	1.4	<	<3	9.9 W,3.1 Ta,0.7 Mo,0.2 C
bond coating powders:								
YHfSi	16.7	12.3	21.6	<	.25	.68	2	0.65Si
Y only	16.6	12.8	23.0	<	<	.42	8	0.04Si

* S in ppmw < indicates less than 0.01 % or 0.0003 % for Y

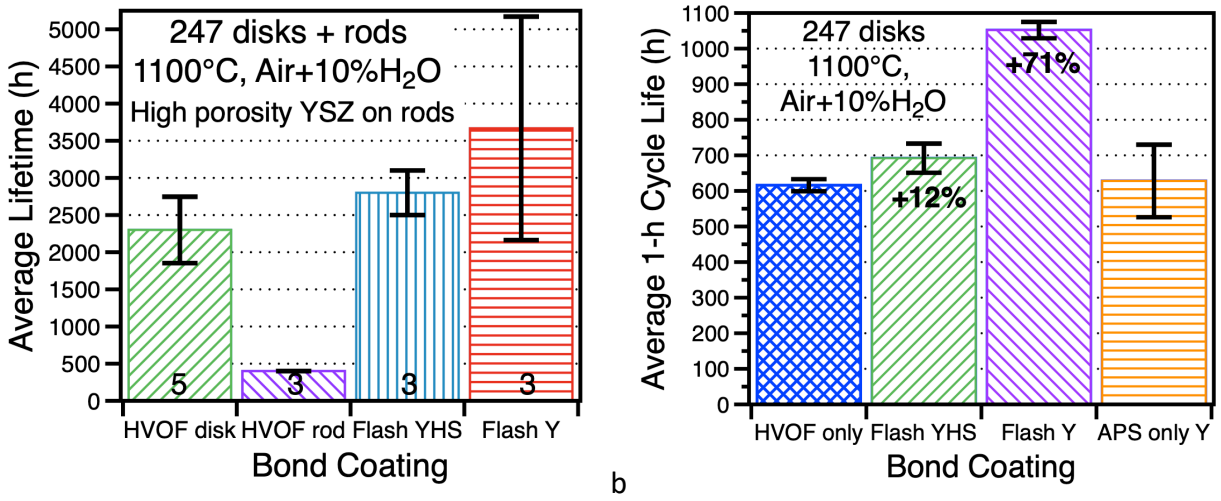

a b

Figure 1. Average coating lifetimes for APS YSZ on 247 substrates with bond coatings of HVOF NiCoCrAlYHfSi with and without APS flash coatings of NiCoCrAlY and NiCoCrAlYHfSi or 100 % APS NiCoCrAlY in furnace cycle testing at 1100 °C in air with 10 % H_2O in (a) 100-h cycles on rod and disk specimens and (b) 1-h cycles on disk specimens. Bars correspond to the average lifetime for 3-5 specimens in (a) and 5 specimens in (b) with whiskers showing one standard deviation. In (b), APS only specimens were part of second batch of specimens. Data from [13,14,25,26].

Results

Figure 1 illustrates the benefit of flash coatings in both 100-hr and 1-hr cycles [13,14,25,26]. For all of the specimens in this series of experiments, the HVOF coating was sprayed using the NiCoCrAlYHfSi powder. The flash coatings were initially recommended by industrial partners for the rod specimens in Figure 1a where the HVOF-only coating resulted in a very short lifetime [13]. The HVOF-only result was particularly surprising because previously five

HVOF-only disk specimens had an average FCT lifetime of ~23, 100-hr cycles suggesting a significant effect of specimen geometry (which is currently being modeled at Stony Brook University to understand this geometry effect). Previous rod results [13] showed a very significant benefit of the flash coating but the APS layer was extremely thick (~200 µm) on the first specimens, such that the increased lifetime could be attributed to a thicker bond coating [25,26]. Figure 1a shows results for a second set of specimens where the flash coatings were 20-30 µm thick and the total bond coating thickness was comparable to the HVOF-only rods (all bond coatings 120-150 µm thick) [25]. In this case, the average lifetimes of the NiCoCrAlY and NiCoCrAlYHfSi flash coatings were not statistically different and were similar to the HVOF-only disk specimens but all were significantly higher than the HVOF-only rods.

The roughness of these flash coatings was reported earlier and the roughness was not as high as reported in a previous study (fractal dimension of 1.07-1.08 vs. 1.31) [11]. Nevertheless, the flash coatings in this study significantly outperformed HVOF-only bond coatings similar to the other study. Characterization of the failed specimens was not as fruitful as hoped, especially because the YSZ spalled at such different times, note the large standard deviation for the flash coatings in Figure 1a.

One way of monitoring the specimens during the test besides mass change was the residual stress in the thermally grown alumina scale. Figure 2 compares the measured compressive stress in a disk specimen with a HVOF bond coating and a rod specimen with a thick (~200 µm) flash coating. The first rod specimen failed at 2100 hr (21 cycles) so a second specimen in the group was tracked at longer times. With the thicker YSZ layer on the rod specimens, the signal through the top coating was much weaker and no statistics on the stress were generated. A lower residual stress was measured in the rod specimens suggesting that more damage accumulated in the rod specimen. However, there were several differences here: (1) substrate geometry, (2) bond coating type and (3) YSZ porosity (higher porosity on the rod specimens, see above). A higher porosity YSZ layer was found to perform better on rod specimens but the difference in porosity was found to affect residual stress with VPS bond coatings [25]. Thus, it is difficult to draw conclusions from these measurements.

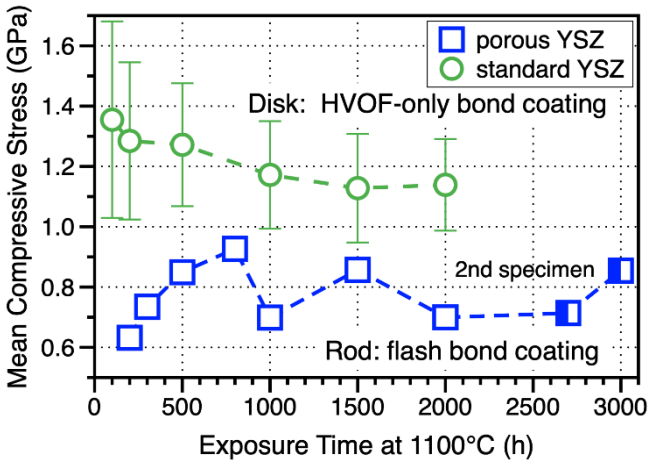

Figure 2. Residual compressive stress in the alumina scale measured by PLPS on 247 disk with HVOF only bond coating and rod specimen with flash coating as a function of exposure time in 100-h cycles at 1100 °C. Additional measurements were made on a second high porosity specimen after the first specimen failed. The whiskers show one standard deviation of the 3468 stress measurements. For the rod, the signal was very weak and all the data were collected into a single spectra and fit so no standard deviation was available. Data from [26].

Figure 1b shows the average FCT lifetime results for 1-hr cycles. In this case, the two flash coatings performed differently with the Y-only flash coating increasing the average FCT lifetime by 71 % compared to an HVOF-only bond coating, while the YHfSi flash coating increased lifetime by 12%. Unlike prior coating batches exploring other parameters [24,29], these results were all statistically significant. The HVOF-only and flash coated specimens were all sprayed in the same batch (HVOF and YSZ) in an attempt to limit coating procedure variability. (The APS-only NiCoCrAlY coatings were part of the second batch discussed below.). As with the rod specimens, the characterization of the failed disk specimens only revealed that the HVOF coating did not fail by Al loss [14]. The flash coating roughness was higher than HVOF (fractal dimension of 1.11-1.13 vs. 1.07 for HVOF only) but, again, much lower than in the previous study [11].

To further understand the benefit of the flash coatings (beyond their marginally higher roughness) and the difference between the two flash coating powders, a suite of characterization techniques was used. However, based on the experience characterizing the failed rod specimens, the characterization focused on a 6th specimen of each coating type (5 were cycled to failure) that was sequentially sectioned during exposure so that clearer comparisons could be achieved. Figure 3 shows the evolution of the two flash coatings from as-received to 500, 1-hr cycles. Both

coatings formed an intermixed metal-oxide zone. At first glance, it does not appear to be a particularly protective microstructure with considerable oxide formation in the intermixed zone.

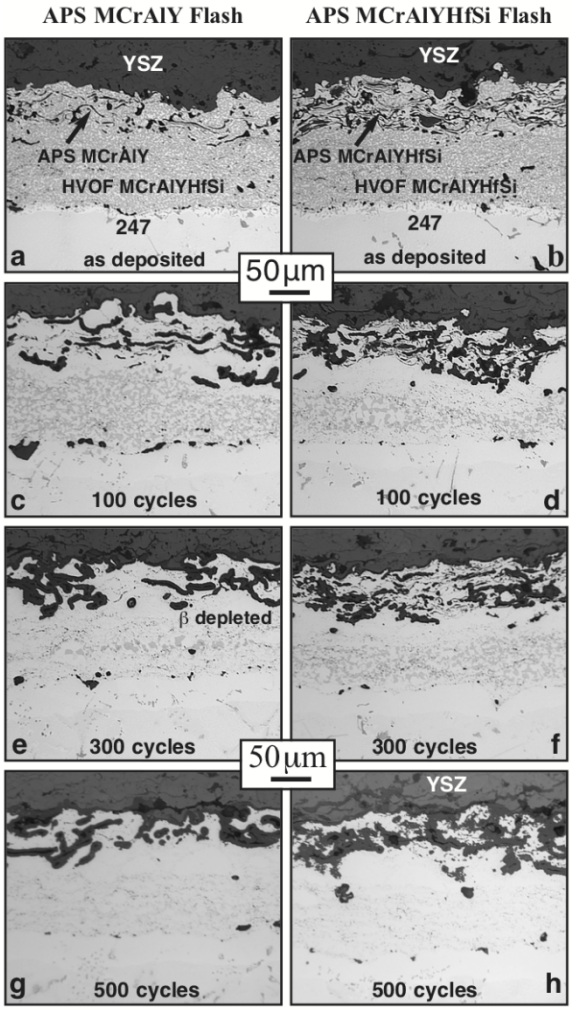

Figure 3. Light microscopy of polished cross-sections of APS flash coated 247 disks with (a,c,e,g) MCrAlY and (b,d,f,h) MCrAlYHfSi, (a,b) as-received, (c,d) after 100, 1-h cycles at 1100 °C in air + 10 % H_2O (e,f) 300 cycles and (g,h) 500 cycles. Both coatings have HVOF MCrAlYHfSi inner layers and YSZ top coatings.

However, this layer may be very effective in inhibiting interfacial crack formation and could act as a graded metal-ceramic interface to reduce stress. In addition to the flash coating increasing the coating roughness, the underlying HVOF layer prevented the oxide from penetrating deeper into the bond coating and acted as a source of Al for this intermixed zone, which could be prone to rapid mixed oxide formation if the metal becomes Al depleted.

Comparing the different behavior of the two flash coatings in Figure 3, the lower Y+Hf content in the Y-only flash coating (Table 1) appeared to minimize oxidation in the flash layer. Even as-annealed, there appeared to be less oxide (darker areas in Figures 3a and 3b) in the Y-only outer layer. As a reminder, the inner layer on both coatings was HVOF NiCoCrAlYHfSi. Rather than the uniform oxide scale formed on an HVOF coating (example shown below), the convoluted intermixed layer continued to grow with an increased oxide volume with time, Figure 3. Based on the contrast in the light microscopy images in Figures 3c-3f, there appeared to be more depletion of the Al-rich β phase with the YHfSi flash coating after 100 and 300 cycles. The β phase appears slightly darker in these images. Since the YHfSi flash coating formed more oxide, greater β depletion is expected. By 500 cycles, no β phase layer is evident in either coating, Figures 3g and 3h. Figure 4 confirms that more β phase remained in the Y only bond coating after 300 cycles using SEM/EDS and the larger oxide volume in the NiCoCrAlYHfSi flash coating resulted in greater Al depletion [14]. Faster Al consumption for the YHSi flash coating could explain the shorter average FCT lifetime in Figure 1b.

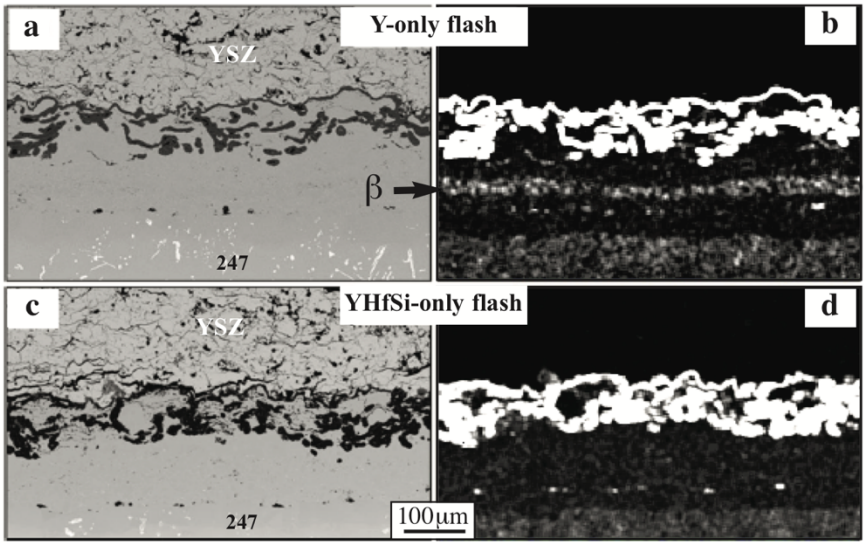

Figure 4. SEM backscattered electron images (a,c) and associated Al EDS maps (b,d) after 300, 1-h cycles at 1100 °C in air+10 % H_2O of (a,b) Y-only flash coating and (c,d) YHfSi flash coating. The β-phase is almost completely depleted in the latter coating. [14]

The same 300 cycle specimens also were characterized using μXCT to further understand the complicated 3D structure of the intermixed zone. Much of the results are qualitative and not

easily presented in a 2D non-color format. However, there appeared to be more interconnected metallic particles in the Y-only flash coating after 300 cycles. Figure 5 attempts to quantify that observation by showing the volume of metal particles remaining in the flash coating layer not directly connected to the underlying HVOF bond coating. The total volume (area under the curve) was almost 6X higher in the NiCoCrAlYHfSi flash coating, which also may suggest an earlier failure when these unconnected particles become Al depleted and oxidized to form voluminous Ni,Cr-rich oxide [30].

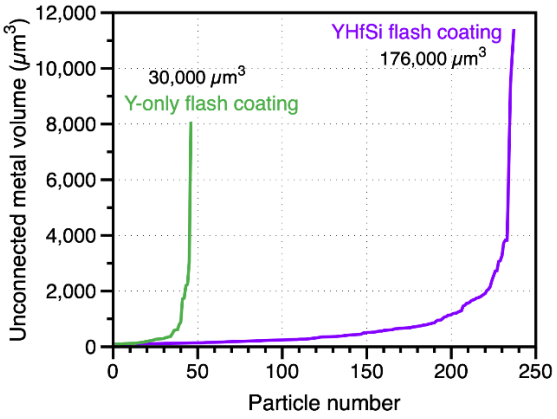

Figure 5. Measured unconnected metal particles in the flash coatings after 300, 1-h cycles at 1100 °C. A much larger number and total volume of particles was measured in the flash coating made with MCrAlYHfSi powder compared to Y-only flash coating.

Another batch of disk specimens is currently being cycled to failure using 1-hr cycles. The same methodology is being used but, in this case, only the NiCoCrAlY powder was used for the HVOF and APS processes and an APS-only bond coating was added for comparison. The APS-only specimens have all failed and showed a similar FCT lifetime as the HVOF-only coatings in the previous batch, Figure 1b. Figure 6 shows cross-sections of the as-annealed coatings and after 100 cycles at 1100 °C. Figure 6a shows the as-annealed HVOF coating and the thin, fairly uniform alumina layer formed after 100 hr is shown in Figure 6b. Figures 6c-6f show a similar set of images for two different Y-only flash coatings with two different flash layer thicknesses. The thicker "flash 1" coating (nominally 50 % of the total bond coating or 50-75 µm) in Figures 6c and 6d resulted in more oxide formation and greater β depletion after only 100 cycles compared to the ~25 % "flash 2" coating (25-50 µm) in Figure 6e-6f. Finally, Figure 6g shows the as-annealed APS-

only bond coating. Not surprisingly, it appeared that oxides had penetrated the entire APS bond coating after only 100 cycles, Figure 6h. For a less oxidation-resistant substrate than a 247 superalloy (e.g. an alloy X combustor liner [31]), this could quickly result in Cr- or Ni-rich oxide formation at the coating-substrate interface.

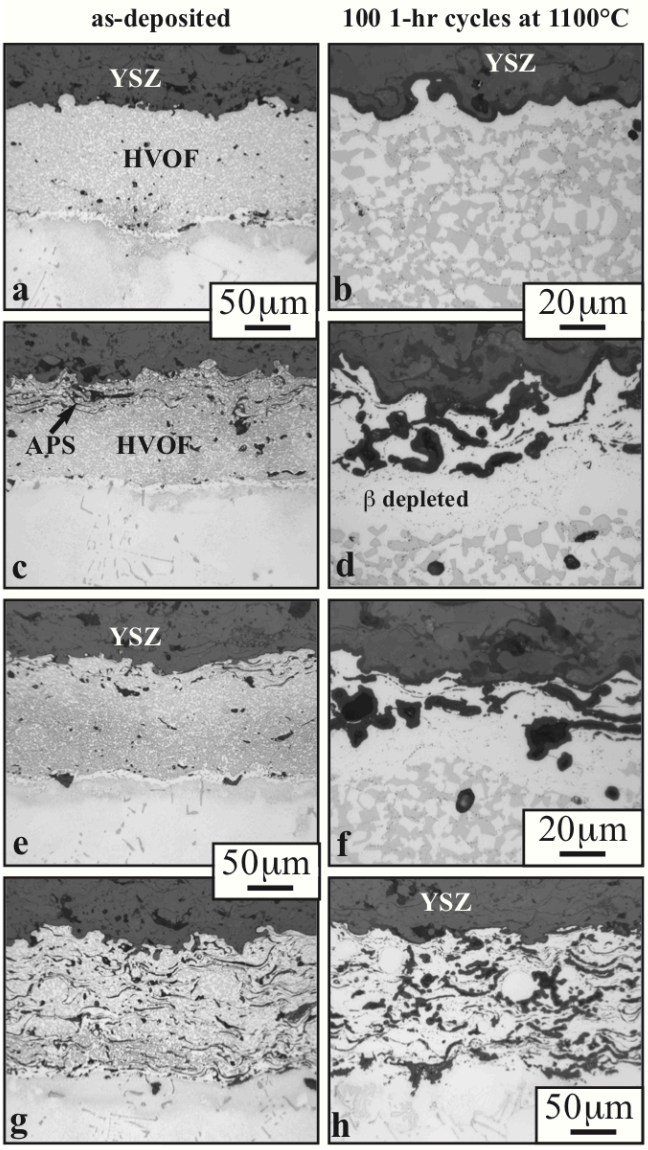

Figure 6. Light microscopy of polished cross-sections of coatings on 247 substrates: (a,c,e,g) as-deposited and (b,d,f,h) after 100, 1-hr cycles at 1100 °C in wet air. (a,b) HVOF bond coating, (c-f) APS outer layer + HVOF inner layer and (g,h) APS bond coating.

Figure 7 shows the average residual stress in one specimen of each coating type measured periodically up to 700, 1-hr cycles when some coating failures began to occur. Similar to prior results [14], the average stress measured on the HVOF-only bond coating dropped faster than

the other coatings. This coated specimen failed after 760 cycles, a slightly longer lifetime than the earlier batch of coatings shown in Figure 1b. The APS-only bond coating started lower than the other specimens but declined more slowly. This particular specimen had a longer lifetime of 800 cycles compared to the average of 628 cycles shown in Figure 1b. Average lifetimes for the flash coatings from this second batch are not yet available.

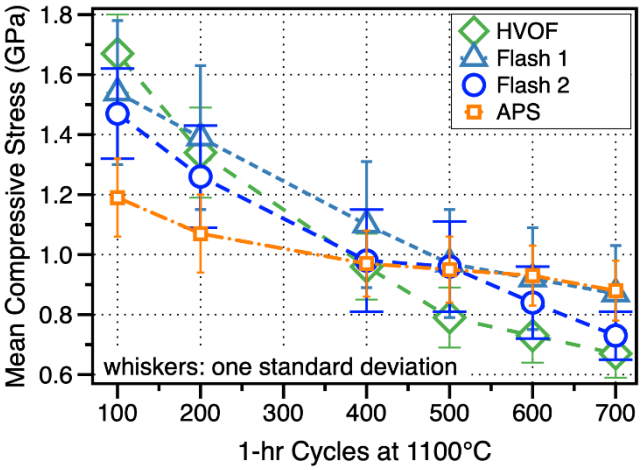

Figure 7. Residual compressive stress in the alumina scale measured by PLPS on 247 disk specimens with different bond coatings shown in Figure 6 as a function of exposure time in 1-h cycles at 1100 °C. Flash 1 refers to Figures 6c-6d and Flash 2 to Figures 6e-6f.

Discussion

New TBC concepts are typically first evaluated in furnace cycle testing (FCT) with thermal gradient testing, such as burner rigs, being used for promising TBC concepts before engine testing [32-34]. The desire to progress onto burner rig testing instigated the switch from disk to rod specimens and the unusual discovery that low roughness HVOF bond coatings performed very poorly on rod specimens, Figure 1a. These FCT results certainly indicate that flash coatings effectively increase TBC lifetime and all indications are that they are widely used in practice. However, the prevailing hypothesis is that their performance is primarily related to their higher roughness, particularly compared to HVOF-only bond coatings. These results indicate that a substantial benefit was gained without a large increase in coating roughness, compared to prior work [11].

Previously, it was found that HVOF-only NiCoCrAlYHfSi bond coatings [4,35] outperformed Y-only bond coatings, similar to results with co-doped wrought alloys [36,37].

Thus, YHfSi powder was used throughout the prior studies on environmental and substrate effects [15,23,24,29]. However, if flash coatings are predicated on improving roughness, then Hf additions to improve alumina scale adhesion should be unnecessary. That hypothesis was proven to be somewhat correct in that there was no benefit of the YHfSi flash coatings but surprisingly the higher Y+Hf content was actually detrimental to coating performance. The lower Y content in the Y-only coating appeared to minimize oxidation in the flash coating layer and result in more interconnected metal, Figure 5. This result supports the observations that coating composition and particularly reactive element additions in MCrAlX powder need to be optimized for the specific coating process [37,38]. The slightly higher S content in the Y-only powder (Table 1) should not play a role as both powders have a Y/S ratio >> 1 [36].

The mechanistic understanding of the flash coating benefit is still in progress. However, given the current results, it must be concluded that it is not just roughness that leads to the benefit. If that were the case, then APS-only and VPS [25] bond coatings should also have a similar beneficial high roughness. Figure 6h shows the importance of the underlying HVOF layer in preventing oxidation from quickly reaching the coating-substrate interface in only 100 cycles at 1100 °C. The HVOF layer prevents the reaction front from penetrating deeper into the coating and quickly consuming the Al reservoir in the coating, resulting a reduced lifetime for the APS-only bond coating compared to the flash coatings. The name “flash” implies that the APS layer on the HVOF bond coating is relatively thin. Figure 6 also begins to suggest that thicker flash layers will simply consume the Al reservoir in the HVOF layer more quickly. However, more characterization is needed in a time series to confirm that observation.

The other role of the HVOF layer is to supply Al to the intermixed alumina-metal zone that effectively consumes the flash coating during exposure. A full proof of this hypothesis is still in progress using SEM/EDS and μXCT. Perhaps serial sectioning using focused ion beam (FIB) milling coupled with EDS also is needed to measure the Al content in the intermixed zone as a function of location and exposure time to confirm. Presumably when the Al is sufficiently consumed in the coating, these small metal ligaments will reach breakaway oxidation and begin forming voluminous Ni- and Cr- rich oxides [30], which will have a rapid negative effect on coating performance. The formation of these mixed oxides has already been observed at flash coating

failure [14], but tracking their evolution through the intermixed zone using μXCT or other means might be insightful for modeling their behavior and optimizing their design and performance. In addition to studying the chemical evolution of flash coatings and their oxidation to understand the failure mechanism and benefit for TBC lifetime, mechanical studies of the interface are needed to understand how the intermixed alumina-metal zone affects the interface properties including crack propagation near the end of life compared to coatings without a flash layer.

Conclusions

Air plasma sprayed flash coatings were very effective in improving TBC lifetime in laboratory FCT evaluations at 1100 °C in air with 10 % H_2O using both 1-hr and 100-hr cycles. The traditional explanation of their benefit is increasing coating roughness compared to HVOF-only bond coatings. They do indeed represent a change in TBC behavior as the optimal NiCoCrAlYHfSi powder for HVOF-only bond coatings is no longer optimal for flash coatings. Flash coatings made with Y-only powder outperformed the YHfSi coatings, where the higher Y+Hf content resulted in more voluminous alumina formation, less interconnected metal in the mixed alumina-metal zone and more rapid β depletion. However, the beneficial effect of flash coatings goes beyond roughness and includes the formation of an alumina-metal mixed zone, which may inhibit crack propagation. In addition, the underlying HVOF layer plays an important role in preventing the mixed zone from growing deeper into the coating and in supplying the mixed zone with Al to delay breakaway oxidation in the mixed zone. A time series of observations has been very effective in identifying these additional effects and is being applied to the second set of Y-only coatings currently being characterized.

Acknowledgments

G. Garner, T. Lowe, T. Jordan, V. Cox assisted with the experimental work at ORNL. This research was sponsored by the U.S. Department of Energy, Office of Fossil Energy, Advanced Turbine Program (R. Dennis program manager and P. Burke project monitor).

References

1. Pint BA (2013) High-Temperature Corrosion in Fossil Fuel Power Generation: Present and Future. JOM 65:1024-1032.
2. Hydrogen-Capable Gas Turbines for Deep Decarbonization. (2019) *EPRI Report* No. 3002017544, Charlotte, NC, Nov. 2019.
3. Michalski J, Bünger U, Crotogino F, Donadei S, Schneider GS, Pregger T, Cao KK, Heide D (2017) Hydrogen generation by electrolysis and storage in salt caverns: Potentials, economics and systems aspects with regard to the German energy transition. Int. J. Hydrogen Energy 42:13427-13443.
4. DeMasi-Marcin JT, Gupta DK (1994) Protective coatings in the gas turbine engine. Surf. Coat. Technol. 68-69:1–9.
5. Goward GW, Progress in Coatings for Gas Turbine Airfoils. Surf. Coat. Technol. 108-109:73-79.
6. Nicholls JR (2003) Advances in Coating Design for High-Performance Gas Turbines. MRS Bulletin 28:659-670.
7. Sahoo P, Carr T, Martin R, Dinh F (1998) Thermal spray manufacturing issues in coating IGT hot section components. J. Thermal Spray Technol. 7:481-483.
8. Nelson WA, Orenstein RM (1997) TBC Experience in Land-Based Gas Turbines. J. Thermal Spray Technol. 6(2):176-180.
9. Stringer J (1998) Coatings in the electricity supply industry: past, present, and opportunities for the future. Surf. Coat. Technol. 108–109:1–9.
10. Subramanian R, Burns A, Stamm W (2008) Advanced Multi-functional Coatings for Land-Based Industrial Gas Turbines," Proc. ASME Turbo Expo 1:549-558.
11. Nowak W, Naumenko D, Mor G, Mor F, Mack DE, Vassen R, Singheiser L, Quadakkers WJ (2014) Effect of processing parameters on MCrAlY bondcoat roughness and lifetime of APS–TBC systems. Surf. Coat. Technol. 260:82–89.
12. Zou Z, Jia L, Yang L, Shan X, Lou L, Guo F, Zhao X, Xiao P (2017) Role of internal oxidation on the failure of air plasma sprayed thermal barrier coatings with a double-layered bond coat. Surf. Coat. Technol. 319:370-377.
13. Pint BA, Lance MJ, Haynes JA (2019) The Effect of Coating Composition and Geometry on TBC Lifetime. J. Eng. Gas Turbine Power 141(3):031004.
14. Lance MJ, Thiesing BP, Haynes JA, Parish CM, Pint BA (2019) The Effect of HVOF Bond Coating with APS Flash Coating on TBC Performance. Oxid. Met. 91:691-704.
15. Gildersleeve EJ, Viswanathan V, Lance MJ, Haynes JA, Pint BA, Sampath S (2019) Role of Bond Coat Processing Methods on the Durability of Plasma Sprayed Thermal Barrier Systems. Surf. Coat. Technol. 375:782-792.
16. Leyens C, Fritscher K, Gehrling R, Peters M, Kaysser WA (1996) Oxide Scale Formation on an MCrAlY Coating in Various H_2-H_2O Atmospheres. Surf. Coat. Technol. 82:133-144.
17. Janakiraman R, Meier GH, Pettit FS (1999) The Effect of Water Vapor on the Oxidation of Alloys that Developed Alumina Scales for Protection. Met. Mater. Trans. 30A:2905-2913.

18. Onal K, Maris-Sida MC, Meier GH, Pettit FS (2003) Water Vapor Effects on the Cyclic Oxidation Resistance of Alumina-Forming Alloys. Mater. High Temp. 20:327-337.
19. Pint BA, Haynes JA, Zhang Y, More KL, Wright IG (2006) The Effect of Water Vapor on the Oxidation Behavior of Ni-Pt-Al Coatings and Alloys. Surf. Coat. Technol. 201:3852-3856.
20. Smialek JL (2008) Enigmatic Moisture Effects on Al_2O_3 Scale and TBC Adhesion. Mater. Sci. Forum, 595-598:191-198.
21. Déneux V, Cadoret Y, Hervier S, Monceau D (2010) Effect of Water Vapor on the Spallation of Thermal Barrier Coating Systems During Laboratory Cyclic Oxidation Testing. Oxid. Metals, 73:83-93.
22. Pint BA, Garner GW, Lowe TM, Haynes JA, Zhang Y (2011) Effect of increased water vapor levels on TBC lifetime with Pt-containing bond coatings. Surf. Coat. Technol. 206:1566-1570.
23. Lance MJ, Unocic KA, Haynes JA, Pint BA (2014) The Effect of Cycle Frequency, H_2O and CO_2 on TBC Lifetime with NiCoCrAlYHfSi Bond Coatings. Surf. Coat. Technol. 260:107-112.
24. Pint BA, Unocic KA, Haynes JA (2016) The Effect of Environment on TBC Lifetime. J. Eng. Gas Turbine Power 138(8):082102.
25. Lance MJ, Thiesing BP, Haynes JA, Gildersleeve EJ, Sampath S, Pint BA, Effect of APS Flash Bond Coatings and Curvature on TBC Performance on Rod Specimens. Surf. Coat. Technol. 378 (2019) 124940.
26. Pint BA, Lance MJ, Haynes JA, Gildersleeve EJ, Sampath S (2020) Effect of APS flash bond coatings on furnace cycle lifetime of disks and rods. J. Eng. Gas Turbine Power in press, https://doi.org/10.1115/1.4046694.
27. Lipkin DM, Clarke DR (1995) Measurement of the stress in oxide scales formed by oxidation of alumina-forming alloys. Oxid. Met. 45:267-280.
28. Buades A, Coll B, Morel JM (2005) A non-local algorithm for image denoising. Paper presented at IEEE Computer Society Conference on Computer Vision and Pattern Recognition, San Diego, California, 20-25 June 2005.
29. Pint BA, Haynes JA, Lance MJ, Aldridge HL, Viswanathan V, Dwivedi G, Sampath S (2016) Factors Affecting TBC Furnace Cycle Lifetime: Temperature, Environment, Structure and Composition. In: Hardy, M et al. (eds.), Superalloys 2016, TMS, Warrendale, PA, 727-734.
30. Evans HE, Taylor MP (2001) Diffusion Cells and Chemical Failure of MCrAlY Bond Coats in Thermal-Barrier Coating Systems. Oxid. Met. 55:17-34.
31. Pint BA, Haynes JA, Besmann TM (2010) Effect of Hf and Y Alloy Additions on Aluminide Coating Performance. Surf. Coat. Technol. 204:3287–3293.
32. Miller RA (1997) Thermal barrier coatings for aircraft engines: History and directions. J. Thermal Spray Technol. 6:35-42.
33. Simms NJ, Kilgallon PJ, Roach C, Oakey JE (2003) Development of oxides at TBC – bond coat interfaces in burner rig exposures. Mater. High Temp. 20:519-526.
34. Mumm DR, Watanabe M, Evans AG, Pfaendtner JA (2004) The influence of test method on failure mechanisms and durability of a thermal barrier system. Acta Materialia 52:1123–1131.

35. Haynes JA, Unocic KA, Pint BA (2013) Effect of Water Vapor on the 1100°C Oxidation Behavior of Plasma-Sprayed TBCs with HVOF NiCoCrAlX Bond Coats. Surf. Coat. Technol. 215:39-45.
36. Pint BA (2003) Optimization of Reactive Element Additions to Improve Oxidation Performance of Alumina-Forming Alloys. J. Amer. Ceram. Soc. 86:686-695
37. Naumenko D, Pint BA, Quadakkers WJ (2016) Current thoughts on reactive element effects in alumina-forming systems - in memory of John Stringer. Oxid. Met. 86:1-43
38. Naumenko D, Pillai R, Chyrkin A, Quadakkers WJ (2017) Overview on Recent Developments of Bondcoats for Plasma-Sprayed Thermal Barrier Coatings. J. Thermal Spray Technol. 26:1743-1757.